This article appeared in The Journal of Chemical Physics **154**, 074703 (2021) and may be found at https://doi.org/10.1063/5.0041273.

Surface Mobility in Amorphous Selenium and Comparison with Organic Molecular Glasses

Jaroslav Barták[1], Jirí Málek[1], Kushal Bagchi[2], M. D. Ediger[2], Yuhui Li[3], Lian Yu[3]*

[1]Department of Physical Chemistry, University of Pardubice, Studentská 573, 53210 Pardubice, Czech Republic

[2]Department of Chemistry, University of Wisconsin-Madison, Madison, Wisconsin 53706, United States

[3]School of Pharmacy, University of Wisconsin–Madison, Madison, Wisconsin 53705, United States

***Corresponding Author**

Jaroslav Barták

Tel: 00420466037043. E-mail: jaroslav.bartak@upce.cz

ORCID: 0000-0001-8675-1144

Abstract

Surface diffusion is important for a broad range of chemical and physical processes that take place at the surfaces of amorphous solids, including surface crystallization. In this work, the temporal evolution of nanoholes is monitored with atomic force microscopy to quantify the surface dynamics of amorphous selenium. In molecular glasses, the surface diffusion coefficient has been shown to scale with surface crystal growth rate (u_s) according to the power relation $u_s \approx D_s^{0.87}$. In this study, we observe, that the same power-law applies to surface crystallization of amorphous selenium, a representative inorganic polymer glass. Our study shows that the surface diffusion coefficient can be used to quantitatively predict surface crystallization rates in a chemically diverse range of materials.

Introduction

Mobility at the surface of amorphous materials plays an important role in processes such as crystallization, sintering, corrosion, and catalysis. There are numerous studies on surface dynamics of polymeric[1-4], molecular[5-10] and inorganic[11-15] glass-forming materials. These papers utilize a range of different methods to study surface diffusion and describe connections to other surface processes, such as surface crystal growth and formation of ultra-stable glasses by vapor deposition. Comparison of surface crystal growth with surface diffusion has a significant impact on the understanding of the crystal growth process, which is important for preparation, processing, and utilization of amorphous materials. In the standard crystal growth models[16], the mobility of the reorganizing structural units is described by a diffusion coefficient. Due to the missing data on temperature dependence of diffusion coefficients for many amorphous materials, they are usually substituted by bulk viscosity via the Stokes-Einstein-Eyring (SEE) equation[17, 18]. The same simplification, using the bulk viscosity data, is often used for crystal growth at surface of bulk samples and thin films, where the experimental data for near-surface viscosity and surface diffusion coefficient are rarer than in bulks. Nevertheless, the SEE relation often breaks down, particularly in the case of lateral crystal growth at surface of bulk samples[19] or in thin films[19-25]. Therefore, a great knowledge of surface self-diffusion is needed for better understanding of crystal growth at surfaces of bulk samples and thin films.

In the past decades, measurements on surface diffusion have been performed in organic glasses by monitoring the flattening of a grating embossed into the surface of the studied materials[1, 2, 5, 8, 9]. This type of experiment is based on measurement of the amplitude change of the (single wavelength) sinusoidal grating, which exponentially decreases with time[9]. Dependence of the decay constant on wavelength of the surface grating reveals the mechanism for the smoothing process[1, 5, 9]. With this approach, several experiments using gratings with different wavelengths are needed to determine the smoothing mechanism. Another way to study surface diffusion is to perform experiments with non-sinusoidal surface profiles. The advantage of this method is, that many Fourier components can be simultaneously probed. Mullins[26] showed that an isolated protrusion or hole can be represented by a sum of its Fourier components, which after individual decay, can be summed again to construct the surface profile at a later time. A surface profile (z) of a protrusion or hole can be described as a function of lateral distance (r) from the hole center and time (t) of annealing, as is shown in Figure 1.

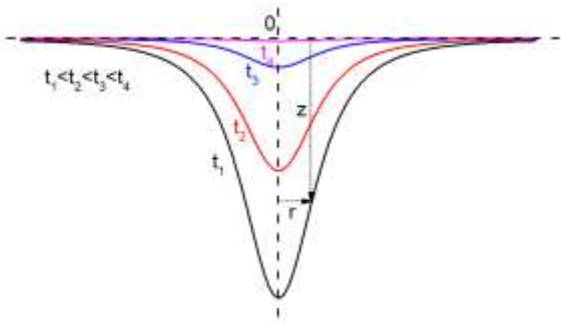

Figure 1 Schematic of flattening of nanohole upon annealing at temperature T for time t

According to Mullins[26], the profile of an isolated hole evolves by different kinetics depending on the mechanism of the flattening process – surface diffusion (eq. 1) or viscous flow (eq. 2):

$$z(r,t) = \frac{a}{8\pi(Bt)^{1/2}} \sum_{n=0}^{\infty} \left[(-1)^n \frac{\Gamma\left(\frac{n+1}{2}\right)}{2^{2n}(n!)^2} \left(\frac{r}{(Bt)^{1/4}} \right)^{2n} \right] \tag{1}$$

$$z(r,t) = \frac{a}{2\pi(Ft)^2 \left(1 + \frac{r}{Ft}\right)^{3/2}} \tag{2}$$

Where a represents the volume of the hole ($a < 0$), and B and F are coefficients from which the surface diffusion coefficient (D_s) and the viscosity (η), respectively, can be calculated:

$$B = \frac{D_s \gamma \Omega^2 \nu}{kT} \tag{3}$$

$$F = \frac{\gamma}{2\eta} \tag{4}$$

The parameter γ corresponds to surface tension, Ω stands for molecular volume and ν is number of molecules per unit area of surface, which can be expressed as $\nu \approx \Omega^{-2/3}$.

In this article, we use the above-mentioned approach of flattening nanoholes to study surface self-diffusion in bulk samples of amorphous selenium (a-Se). Selenium is a monoatomic chalcogenide glass-former which can form chains, thus, making it intermediate between polymeric and molecular glasses. Due to its photoconducting nature, a-Se is of interest in the photocopying industry[27]. Recently, a-Se has found application in direct conversion flat panel X-ray imagers used in security and medicine[28, 29]. This is the first work reporting direct measurements of surface self-diffusion in chalcogenide glass-forming materials. Here we show that crystal growth rate in amorphous selenium, as a representative of inorganic polymer glass-former, obeys the same power law relation with surface diffusion (with the same exponent) as

organic glass-formers. This is important for understanding and predicting the fast surface crystallization in these materials.

Materials and experimental methods

Samples of glassy selenium were prepared by classical melt-quench method from pure selenium (6N purity, HiChem, Prague, CZ). Pure selenium was placed into a clean quartz ampule. The ampule was evacuated to a pressure of 10^{-3} Pa and sealed to prevent oxidation during melting. The evacuated ampule was placed into a rocking furnace and heated up to 500 °C afterwards. The ampule was held at 500 °C for 20 hours and then the temperature was lowered to 350 °C. Afterwards, the ampule was taken out of the furnace and cooled down to room temperature in the flowing air. The prepared bulk samples were confirmed to be amorphous by optical microscopy (Olympus X51 equipped with camera DP72) and by x-ray diffraction analysis (Bruker AXS X-ray diffractometer D8 Advance).

Bulk samples were then cut to small pieces (5 mm cubes) and grained and polished to optical quality with the final thickness of approximately 1 mm. The preparation of nanoholes on surface of amorphous materials was described in the thesis of Ruan[30] by placing the back side of a plastic holographic grating (Rainbow Symphony Inc.) onto the amorphous material surface at temperature above T_g. In the same way the nanoholes were prepared on surface of polished selenium samples at 55 °C (T_g = 30 °C). The sample was then cooled to room temperature and the plastic was peeled off. The back side of the plastic holographic gratings contained protrusions which were used to create nanoholes on the surface of a-Se. The structure on the samples surface was characterized by atomic force microscopy (AFM, Multimode8HR, Bruker Nano Inc.). To follow the evolution of nanoholes profiles in time, the samples were annealed at different temperatures (25 – 40 °C) in a brass furnace with temperature stability of ± 0.1 °C. The annealing was performed ex-situ and at every time of AFM measurement, the samples were cooled down to 20 °C and scanned by AFM in taping mode.

Results and discussion

This article focuses on measurement of the surface diffusion coefficient (D_s) of amorphous selenium (a-Se) using temporal evolution of nanoholes embossed onto the surface of bulk samples. The nanoholes were prepared by embossing as described above. The samples were isothermally annealed at different temperatures in the range of 25 – 40 °C and the temporal evolution of nanohole profiles monitored using atomic force microscope (AFM) in tapping mode. In Figure 2, the temporal evolution of an isolated hole of ca 200 nm in diameter is shown.

The sample was annealed at 25 °C and during the annealing the nanohole was filled by the surrounding material. The AFM images were transformed to the height profile (z) as a function of hole radius (r) and time (t). The radius was calculated from AFM image as lateral distance from the center of the hole, and the data were plotted as $z = f(r,t)$ (Figure 2). For every sample 5-10 nanoholes with diameters in the range of 100 – 300 nm were scanned and analyzed.

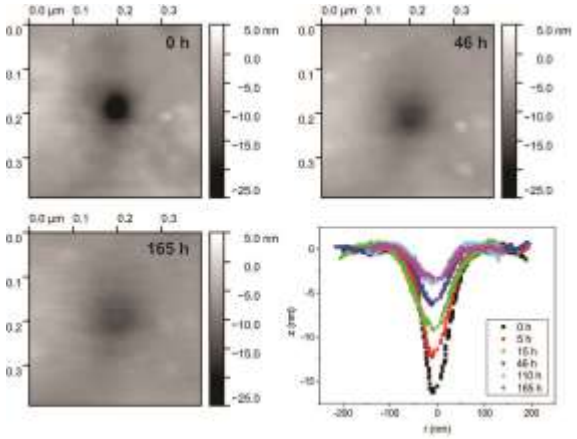

Figure 2 Temporal evolution of a nanohole profile on surface of a-Se at 25 °C

To determine the mechanism for the filling process, one method is to follow the temporal evolution of the depth of the hole (minimal z at $r = 0$). For the two filling mechanisms described by eqs. 1 and 2, we obtain:

$$z_{\min}(0,t) = \frac{a\,\Gamma\left(\frac{1}{2}\right)}{8\pi(Bt)^{1/2}} \tag{5}$$

$$z_{\min}(0,t) = \frac{a}{2\pi(Ft)^{2}} \tag{6}$$

Plotting the dependence of $z_{\min}^{-2}$ and $z_{\min}^{-1/2}$ on t reveals the mechanism responsible for hole filling (surface diffusion or viscous flow). If $z_{\min}^{-2}$ is linear on t the filling process occurs by surface diffusion. On the other hand, if $z_{\min}^{-1/2}$ is linear on t, the filling process occurs by viscous flow. Here it is important to note, that the time t in eqs. 1,2 and 5,6 should be expressed as $t = t_{exp} + t_0$, where t_{exp} is the actual experimental time and t_0 is an offset time, that is, the time needed for an infinitely sharp and deep hole (a delta function) to evolve to the first recorded profile[26]. The time t_0 can be also evaluated from the linear dependences of $z_{\min}^{-2}$ or $z_{\min}^{-1/2}$ on t_{exp} for the process driven by surface diffusion or viscous flow, respectively.

Analysis of experimental data taken on time evolution of nanohole profile in a-Se is shown in Figure 3. The temporal evolution of z_{min}^{-2} and $z_{min}^{-1/2}$ was calculated and plotted for each measured nanohole to determine the mechanism for the nanohole filling process, as is shown in Figure 3b and 3e. From the linear dependence of z_{min}^{-2} or $z_{min}^{-1/2}$ on the experimental time t_{exp}, the offset time t_0 was calculated as the intersection of the achieved linear dependence with t_{exp}-axis, with the intersection corresponding to $-t_0$. We observe, that for temperatures $T < 35$ °C the filling process occurs by surface diffusion resulting in a linear dependence of z_{min}^{-2} on t_{exp}. On the other hand, for temperatures $T > 35$ °C the filling process occurs by viscous flow, as seen from the linear dependence of $z_{min}^{-1/2}$ on t_{exp}. Interestingly, at the temperature $T = 35$°C, some nanoholes showed filling by surface diffusion, while others by viscous flow, indicating this is the temperature at which the surface evolution mechanism changes.

When the proper mechanism of hole filling is known, all data should collapse to a master curve when plotting $z \cdot t^{1/2}$ vs. $r/t^{1/4}$ for the surface diffusion model and plotting $z \cdot t^2$ vs. r/t for the viscous flow model. This collapse to master curve was indeed observed, as is shown in Figure 3c and 3f for the surface diffusion model and the viscous flow model, respectively. Furthermore, each master curve can be fitted by the appropriate model (eq. 1 or 2). The fitting yields a (the volume of the hole) and B (mass transfer constant for surface diffusion, eq. 1) or F (mass transfer constant for viscous flow, eq. 2). From the parameters B and F the surface diffusion coefficient (eq. 3) and viscosity (eq. 4) can be calculated. This calculation requires surface tension γ and molecular volume Ω for a-Se. The temperature dependence of surface tension in selenium melt, undercooled melt and glass was reported by Lee[31]; in the studied temperature range of 25 – 40 °C, the surface tension varies in the range of 124 – 126 mN/m. Molecular volume of a-Se was calculated from specific volume V_{sp} reported by Berg and Simha[32], molar mass M of Se and Avogadro's constant N_A: $\Omega = V_{sp} \cdot M/N_A$. The molecular mass M of the transported structural units during the diffusion process is somewhat uncertain because of polymeric structure of a-Se which is composed of chains of different lengths and rings[33-37]. At present, there is very little known about the molecular weight distribution in a-Se. Faivre and Gardissat[33] reported that a-Se has a relatively low degree of polymerization and a narrow molecular weight distribution. For simpicitya the monomer is assumed to be the diffusing unit. Using the data of V_{sp} published by Berg and Simha[32] the molecular volume Ω is 0.0307 – 0.0309 nm^3 in the studied temperature range of 25 – 40 °C. The obtained values of Ω are in good agreement with molecular dynamics simulation of selenium performed by Caprion and Schober[35, 36].

With knowledge of γ and Ω, the surface diffusion coefficients were evaluated, and the results are shown in the Table 1 in the temperature range of 25 – 35 °C. At the temperature higher than 35 °C, the measured data on nanohole filling only viscous flow the smoothing mechanism. On the other hand, below 35 °C filling process occurred by surface diffusion. At 35 °C, larger holes (diameter > 250 nm) provided data on filling by viscous flow and smaller holes (diameter < 200 nm) provided data on filling by surface diffusion. The coefficients of D_s and η found in this way are listed in Table 1.

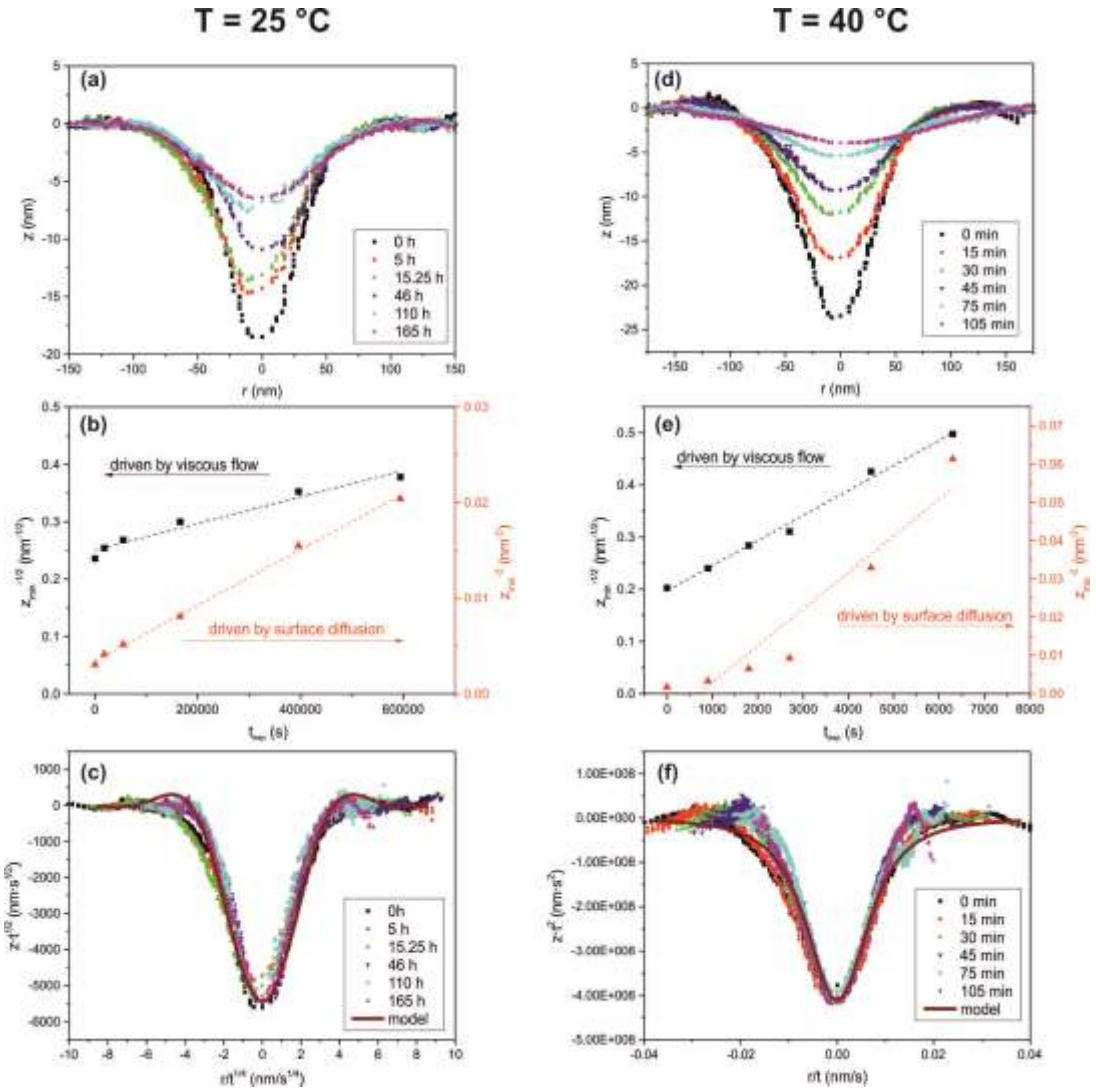

Figure 3 Temporal evolution of nanohole profiles at 25 °C (a) and 40 °C (d). (b, e) Assessment of the mechanism of nanohole filling and the offset time t_0 (see the text for more details). Scaled master curves for nanohole filling by the surface diffusion model according to eq. 1 (c) and viscous flow model according to eq. 2 (f) (see the text for more details).

Table 1 Surface diffusion coefficients (D_s) and viscosity (η) of a-Se at different temperatures

T (°C)	log (D_S / $m^2 \cdot s^{-1}$)	log (η / Pa·s)
25	-17.31 ± 0.16	–
30	-16.67 ± 0.17	–
35	-16.06 ± 0.14	10.11 ± 0.19
40	–	9.79 ± 0.15

The viscosity data measured from the nanohole filling experiments represent the viscosity in the top tens of nanometers of a-Se (depth of the nanoholes). It is of interest to compare these values with viscosity data measured in bulk a-Se by other experimental techniques (Figure 4) and summarized in the work of Koštál and Málek[38]. The near surface viscosity agrees well with the viscosity of bulk material.

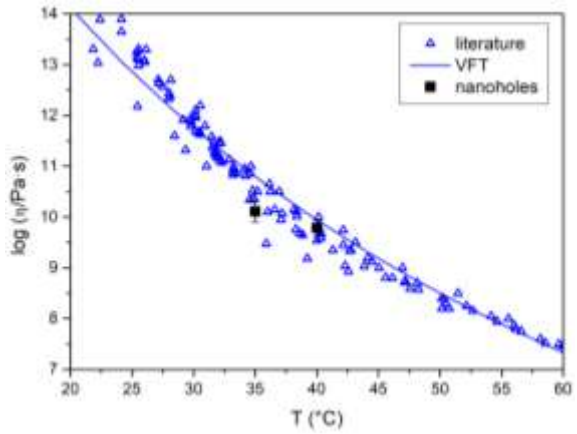

Figure 4 Surface viscosity of amorphous selenium. Near surface viscosity is obtained from temporal evolution of nanoholes on the surface of a-Se and is compared with bulk viscosity reported in the literature[38]. A fit to the Vogel-Fulcher-Tammann (VFT) model is shown by the solid line.

The measurements of nanohole filling in this work have provided the first surface diffusion coefficients of a-Se (Table 1). We find these values are significantly smaller than those of molecular glasses (Figure 5). This is consistent with the notion that the polymers have slower surface diffusion than small molecules, a consequence of the penetration of chain molecules into the bulk where mobility is low[1, 6]. The polymerization of selenium atoms means part of the molecule could be anchored deep into the bulk, limiting its surface diffusion. This is consistent with work recently published by Zhang et al.[39]. Based on structure and stability measurements of vapor deposited a-Se films, they inferred that surface mobility in a-Se thin films is low and rationalized this on the basis of the polymeric nature of a-Se. The surface diffusion coefficients

determined here enables a comparison with the surface crystal growth rate in a-Se. Huang et al.[5] showed, that in molecular glasses, there is a strong correlation between the surface diffusion coefficient and surface crystal growth rate (u_s), which can be expressed as $u_s \approx D_s^{0.87}$ (Figure 5). The temperature dependence of surface crystal growth rate was studied in our previous work[19]. The results of this work enable a test of whether the relation holds also for a-Se. In Figure 5, the calculated crystal growth rates are plotted against the measured surface diffusion coefficient (Table 1). It is clear, that the proposed dependence of $u_s \approx D_s^{0.87}$ holds also for a-Se, which means that the surface lateral growth occurs by surface diffusion. This conclusion is qualitatively consistent with previous measurements[19] that show the surface lateral crystal growth rate in a-Se deviates significantly from the bulk viscosity. It is particularly striking that the dependence of $u_s \approx D_s^{0.87}$ holds not only in molecular glasses but also in inorganic selenium, which can be considered due to its polymeric structure as a bridge between molecular glasses and polymers. Moreover, if the dependence of $u_s \approx D_s^{0.87}$ can be generalized for a broad range of materials, this could be of great importance, because from the knowledge of surface diffusion, the crystallization rate can be estimated. Conversely, from surface crystal growth rates (often easier to measure) the surface diffusion rate can be assessed. The measurement of molecular glasses summarized in Figure 5 and present study of a-Se can be the first steps of such generalization.

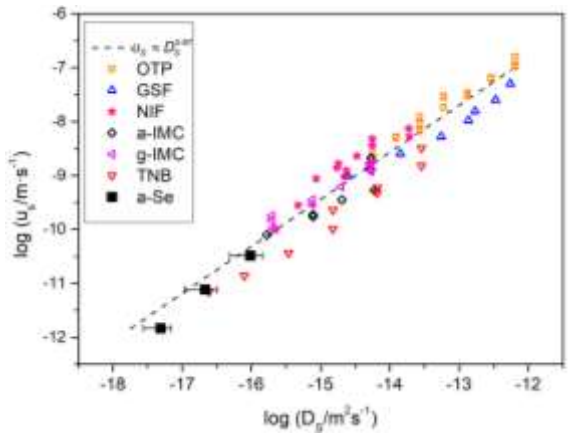

Figure 5 Surface crystal growth rate (u_s) as a function of surface diffusion coefficient (D_s) in a-Se (present data) and molecular glass-formers: o-terphenyl (OTP)[40], griseofulvin (GSF)[5], nifedipine (NIF)[40], α- and γ-indomethacin (IMC)[40] and tris-napthyl benzene (TNB)[7]. Surface crystal growth rates in all the glass-formers are well described by the same power law relation to the surface diffusion coefficient: $u_s \approx D_s^{0.87}$.

Conclusion

In this study, the temporal evolution of nanoholes embossed onto the surface of amorphous selenium was monitored by atomic force microscopy. Samples were isothermally annealed in the range of 25 – 40 °C. At temperatures above 35 °C, the filling process occurs by viscous flow. The viscosity near the surface probed by nanoholes is the same as the bulk viscosity. At temperatures below 35 °C, the filling of nanoholes occurs by surface diffusion. At these temperatures, the surface diffusion coefficient could be measured. Importantly, the surface diffusion coefficient scales with the surface crystal growth rate obeying the power law observed for molecular glasses: $u_s \approx D_s^{0.87}$. Our findings suggest the general validity of this power law ($u_s \approx D_s^{0.87}$) across different types of glass-forming materials.

Acknowledgements

This research was supported by the Czech Science Foundation under grant no. 20-02183Y and the US National Science Foundation (NSF) through the University of Wisconsin Materials Research Science and Engineering Center under grant DMR-1720415.

Availability of data

The data that support the findings of this study are available from the corresponding author upon reasonable request.

References

[1] W. Zhang, and L. Yu, Macromolecules **49**, 731 (2016).

[2] W. Zhang, C. W. Brian, and L. Yu, J. Phys. Chem. B **119**, 5071 (2015).

[3] Y. Chai *et al.*, Science **343**, 994 (2014).

[4] Z. Fakhraai, and J. A. Forrest, Science **319**, 600 (2008).

[5] C. B. Huang *et al.*, J. Phys. Chem. B **121**, 9463 (2017).

[6] Y. H. Li *et al.*, Soft Matter. **16**, 5062 (2020).

[7] S. Ruan *et al.*, J. Chem. Phys. **145**, 064503 (2016).

[8] L. Yu, Adv. Drug Deliver. Rev. **100**, 3 (2016).

[9] L. Zhu *et al.*, Phys. Rev. Lett. **106**, 256103 (2011).

[10] S. Ruan *et al.*, The Journal of Chemical Physics **146**, 203324 (2017).

[11] J. M. Sallese *et al.*, J. Appl. Phys. **88**, 5751 (2000).

[12] D. Llera-Hurlburt, A. S. Dalton, and E. G. Seebauer, Surf. Sci. **504**, 244 (2002).

[13] A. S. Dalton, Y. V. Kondratenko, and E. G. Seebauer, Chem. Eng. Sci. **65**, 2172 (2010).

[14] C. R. Cao *et al.*, App.l Phys. Lett. **107**, 141606 (2015).

[15] C. R. Cao, L. Yu, and J. H. Perepezko, App.l Phys. Lett. **116**, 231601 (2020).

[16] K. A. Jackson, D. R. Uhlmann, and J. D. Hunt, J. Cryst. Growth **1**, 1 (1967).

[17] D. R. Uhlmann, *Crystal growth in glass forming system* (American Ceramics Society, Ohio, 1972), Advances in Nucleation and Crystallization in Glasses, 91-115.

[18] I. S. Gutzow, and J. W. P. Schmelzer, *The Vitreous State: Thermodynamics, Structure, Rheology, and Crystallization* (Springer Berlin Heidelberg, 2013),

[19] J. Barták *et al.*, Cryst. Growth Des. **18**, 4103 (2018).

[20] J. Barták, and J. Málek, J. Therm. Anal. Calorim. **110**, 275 (2012).

[21] J. Barták *et al.*, J. Appl. Phys. **115**, 123506 (2014).

[22] J. Barták *et al.*, J. Non-Cryst. Solids **410**, 7 (2015).

[23] S. Martinkova *et al.*, J. Phys. Chem. B **121**, 7978 (2017).

[24] S. Martinkova *et al.*, J. Appl. Phys. **120**, 145301 (2016).

[25] V. Podzemna, J. Bartak, and J. Malek, J. Therm. Anal. Calorim. **118**, 775 (2014).

[26] W. W. Mullins, J. Appl. Phys. **30**, 77 (1959).

[27] B. Paris, US Patent 2,803,541 (1957)

[28] S. Kasap *et al.*, Sensors **11**, 5112 (2011).

[29] W. Zhao *et al.*, Nuclear Instruments and Methods in Physics Research Section A: Accelerators, Spectrometers, Detectors and Associated Equipment **549**, 205 (2005).

[30] S. Ruan, (University of Wisconsin-Madison, Madison, Wiscosin, USA, 2017), p. 103.

[31] L.-H. Lee, J. Non-Cryst. Solids **6**, 213 (1971).

[32] J. I. Berg, and R. Simha, J. Non-Cryst. Solids **22**, 1 (1976).

[33] G. Faivre, and J. L. Gardissat, Macromolecules **19**, 1988 (1986).

[34] A. Eisenberg, and A. V. Tobolsky, Journal of Polymer Science **46**, 19 (1960).

[35] D. Caprion, and H. R. Schober, J. Non-Cryst. Solids **326**, 369 (2003).

[36] D. Caprion, and H. R. Schober, Phys Rev B **62**, 3709 (2000).

[37] A. H. Goldan *et al.*, J. Appl. Phys. **120**, 135101 (2016).

[38] P. Koštál, and J. Málek, J. Non-Cryst. Solids **356**, 2803 (2010).

[39] A. Zhang *et al.*, Proceedings of the National Academy of Sciences **117**, 24076 (2020).

[40] M. Hasebe *et al.*, J. Phys. Chem. B **118**, 7638 (2014).